# Line Formation of a Normal Zeeman Triplet

Wasaburo UNNO

*Department of Astronomy, University of Tokyo*

(Received August 14, 1956)

Abstract

Line formation of a normal Zeeman triplet is investigated. The equations of transfer for the Stokes Parameters are solved with special regard to the polarization of the Zeeman components. The magnetic field is assumed to be homogeneous, but the orientation of the line of force is not specified. The magnetic intensification and the polarization of the lines are calculated. The magnetic intensification is maximum when the magnetic lines of force make an angle about 55° with the line of sight in the case of well separated triplet.

The method of determining the orientation of the magnetic lines of force are described. The errors introduced by the atmospheric scintillation can advantageously be corrected in this method. An application of the method to the magnetic field of a sun-spot is discussed.

## 1. *Introduction.*

The sun-spot and several magnetic stars are known to have strong magnetic field of a few thousand gauss near the surface. Absorption lines which have large Landé factors split into Zeeman components. The separation of these components is of the order of magnitude of the Doppler width both in the spectra of sun-spots and magnetic stars. Therefore, the appreciable magnetic intensification and polarization of absorption lines will result.

Theoretical calculation of the intensity and the polarization of the absorption line can easily be made when the separations of the Zeeman components are so large that they can be treated as independent lines or when the magnetic lines of force are parallel or perpendicular to the line of sight. The former case was treated by H. W. Babcock[1] both for normal and anomalous Zeeman effect. While, the latter cases called the longitudinal and the transverse Zeeman effects, respectively, were treated by H. Hubenet[2] when the magnetic fields were possibly inhomogeneous. The intensities and the polarizations along the line contour of blended Zeeman components are calculated in this paper when the homogeneous magnetic field has an arbitrary orientation.

The magnetic field is of primary importance in the physics of the sun-spots. But the three dimensional structure of the sun-spot magnetic field is rather obscure. J. Houtgast and A. van Sluiters[3] determined the variation of the magnetic field strength with the depth, statistically, from the center-limb variation of field intensities. G. E. Hale and S. B. Nicholson[4] observed the transverse Zeeman effect in the sun-spots at the limb of the sun and determined the projected direction of the lines of the magnetic field by measuring the angle of the Nicol prism with which the $\sigma$ and $\pi$ components of the Zeeman triplet show their maximum contrast. These methods, when applied to the penumbra or to the outer part of the umbra of sun-spots, cannot escape from the errors introduced by the atmospheric .scintillations. A new method in which the errors can be corrected will be discussed later.

The curve of growth of a sun-spot is different whether the absorption lines are subject to the magnetic intensification or not. P. ten Bruggencate and H. von Klüber[5)] assumed the maximum magnetic intensification in their interpretation of the curve of growth. But, in the longitudinal normal Zeeman effect, we have no magnetic intensifications as Hubenet stated. Therefore, R. Michard[6)] neglected it altogether. J. Warwick[7)] studied it empirically and found no indication of magnetic intensifibation even in the anomalous Zeeman lines. As the angle between the magnetic lines of force and the line of sight increases, the magnetic intensification increases and reaches its maximum when the angle is near 55° and then decreases slightly.

Some of the discussions about the sun-spot may also be applicable to the magnetic stars.

## 2. *The Representation of Polarized Light and the Equation of Radiative Transfer.*

When the angle between the magnetic line of force and the line of sight is arbitrary, the strength and the polarization of the absorption coefficient of each Zeeman component are the functions of the angle, and moreover the polarizations of components are neither identical nor independent to each other. Therefore, if the components are blended, the radiative transfer cannot be treated by the usual polarization optics. A general procedure such as S. Chandrasekhar[8)] applied to the Rayleigh scattering atmosphere must be used. That is the radiative transfer of the Stokes parameters.

In order to obtain the transfer equations for the Stokes parameters, we shall work with a representative polarized light. A Cartesian coordinate system is used as is shown in Fig. 1. $z$-axis is in the direction of propagation of the light, and $x$-axis is in the plane which is determined by the $z$-axis and the magnetic line of force OH. And $y$-axis is taken to be perpendicular to both $z$ and $x$-axis.

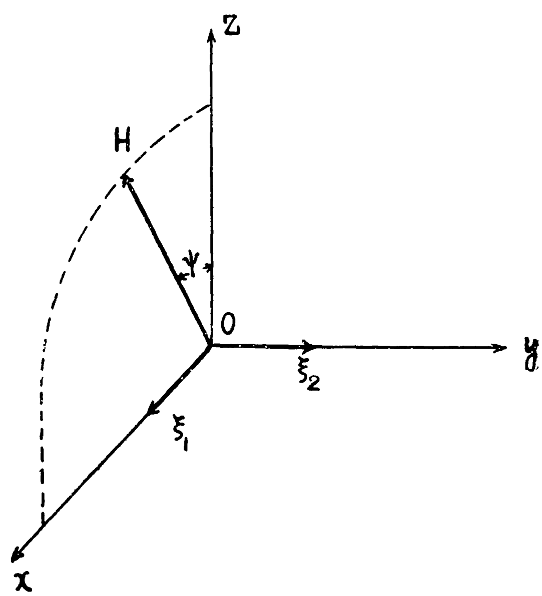


Fig. 1. Coordinate system for representing the polarization. $z$-axis shows the direction of propagation or the direction of the line of sight. The magnetic line of force OH is in the $z-x$ plane and $\psi$ is the angle $z$OH.

A representative polarized light is defined dy

$$\xi_x = \xi_1 \cos(\omega t - \epsilon_1)\,, \qquad (1, a)$$

and

$$\xi_y = \xi_2 \cos(\omega t - \epsilon_2)\,, \qquad (1, b)$$

where $\xi_x$ and $\xi_y$ denote the vibrations of the electric vector of the light along the $x$ and the $y$-axes, respectively, and are defined by the amplitudes $\xi_1$ and $\xi_2$ and the the phase angles $\epsilon_1$ and $\epsilon_2$. The Stokes parameters of the light are sufficient to describe the full nature of polarization and are given by

$$\boldsymbol{I}=(I, Q, U, V), \tag{2, a}$$

where

$$I=I_1+I_2\,, \qquad Q=I_1-I_2\,, \tag{2, b}$$

$$I_1=\overline{\xi_1^2}\,, \qquad I_2=\overline{\xi_2^2}\,, \tag{2, c}$$

$$U=2\overline{\xi_1\xi_2\cos(\epsilon_1-\epsilon_2)}\,, \tag{2, d}$$

$$V=2\overline{\xi_1\xi_2\sin(\epsilon_1-\epsilon_2)}\,. \tag{2, e}$$

According to the classical theory of Lorentz, the absorbing and the emitting electrons are assumed to be linear oscillators. In the presence of magnetic field, all the linear oscillators undergo the precession around the magnetic line of force and they are equivalent to linear oscillators with the original frequency along the line of force plus the left-handed and right-handed circular oscillators with the corresponding shifts in frequency in the plane perpendicular to the line of force, and these oscillators produce the $\pi$-component and the $\sigma$-components, respectively. They are denoted here by $p$-, $l$- and $r$-electrons, respectively. We shall first formulate the selective absorption due to these electrons.

Let $\kappa_p$, $\kappa_l$ and $\kappa_r$ be the absorption coefficients per unit volume per unit solid angle for the radiations with their resonance polarizations, respectively. For instance, if the radiation with the left-handed circular polarization propagates along the magnetic line of force, the intensity $I$ undergoes the absorption $\kappa_l I dz$ after passing the distance $dz$. We have

$$\kappa_p(\nu)=\kappa_l(\nu\mp\varDelta\nu_H)=\kappa_r(\nu\pm\varDelta\nu_H)=\kappa_\nu\,, \tag{3, a}$$

$$\eta_p=\kappa_p/\kappa\,, \quad \eta_l=\kappa_l/\kappa \quad \text{and} \quad \eta_r=\kappa_r/\kappa\,, \tag{3, b}$$

for the normal Zeeman triplet, where $\varDelta\nu_H$ represents the frequency shift due to the Zeeman effect, $\kappa_\nu$ is the usual absorption coefficient when the magnetic field is absent, and $\kappa$ is the continuous absorption coefficient.

The radiations of the resonance polarizations for the polarized oscillators have to be picked up from the system which is represented by the equations (1) and (2).

The $p$-electrons absorb the electric vibration parallel to the magnetic field. The effective absorption coefficient is $\kappa_p \sin^2\psi$. After passing a distance $\varDelta z$, the change in intensity will be

$$\varDelta I_1=-\kappa_p\sin^2\psi I_1\varDelta z\,. \tag{4}$$

From the equations (2) and (4), we have

$$\Delta\xi_1^2 = -\kappa_p \sin^2\psi\,\xi_1^2\Delta z\,,$$

or

$$\Delta\xi_1 = -\frac{1}{2}\kappa_p \sin^2\psi\,\xi_1\Delta z\,. \tag{5}$$

So, the changes in the system (2) are given by

$$\Delta I_1 = -\kappa_p\Delta z\sin^2\psi I_1\,, \tag{6, a}$$

$$\Delta I_2 = 0\,, \tag{6, b}$$

$$\Delta U = -\frac{\kappa_p}{2}\Delta z\sin^2\psi U\,, \qquad (p\text{-absorption}) \tag{6, c}$$

and

$$\Delta V = -\frac{\kappa_p}{2}\Delta z\sin^2\psi V\,. \tag{6, d}$$

The calculation of the absorption due to the $l$-electrons or the $r$-electrons requires some considerations. The $l$-electrons absorb the elliptically polarized radiation, the $l$-radiation which is represented by

$$\xi_{lx} = a\cos\psi\cos(\omega t-\delta_1)\,, \tag{7, a}$$

and

$$\xi_{ly} = a\cos(\omega t-\delta_1-\pi/2)\,, \tag{7, b}$$

but they cannot affect the oppositely polarized radiation represented by

$$\xi_{lx}^* = b\cos(\omega t-\delta_2)\,, \tag{8, a}$$

and

$$\xi_{ly}^* = b\cos\psi\cos(\omega t-\delta_2+\pi/2)\,. \tag{8, b}$$

The system represented by the equations (7) and (8) together must be equivalent to the system represented by the equations (1). So, we have

$$\xi_x = \xi_{lx} + \xi_{lx}^*\,, \tag{9, a}$$

and

$$\xi_y = \xi_{ly} + \xi_{ly}^*\,, \tag{9, b}$$

From the equations (2) and (9),

$$a^2 = \frac{1}{(1+\cos^2\psi)^2}\left[I_1\cos^2\psi + I_2 - V\cos\psi\right]\,, \tag{10, a}$$

$$b^2 = \frac{1}{(1+\cos^2\psi)^2}\left[I_1 + I_2\cos^2\psi + V\cos\psi\right]\,, \tag{10, b}$$

$$I_1=a^2\cos^2\psi+b^2+2ab\cos\psi\cos(\delta_1-\delta_2)\,, \tag{11, a}$$

$$I_2=a^2+b^2\cos^2\psi-2ab\cos\psi\cos(\delta_1-\delta_2)\,, \tag{11, b}$$

$$U=-2ab(1+\cos^2\psi)\sin(\delta_1-\delta_2)\,, \tag{11, c}$$

and

$$V=2[-a^2\cos\psi+b^2\cos\psi-ab\cos(\delta_1-\delta_2)\sin^2\psi]\,. \tag{11, d}$$

$a^2$, $b^2$, $2ab\cos(\delta_1-\delta_2)$ and $2ab\sin(\delta_1-\delta_2)$ can be regarded as the generalized Stokes parameters. In the system (10) and (11), only the intensity of the $l$-radiation, $a^2$, is changed by the absorption due to the $l$-electrons, so that,

$$\varDelta a^2=-\kappa_l\frac{1+\cos^2\psi}{2}a^2\varDelta z\,, \tag{12, a}$$

or

$$\varDelta a=-\frac{\kappa_l}{4}\varDelta z(1+\cos^2\psi)a\varDelta z\,, \tag{12, b}$$

where $\kappa_l(1+\cos^2\psi)/2$ is the effective absorption coefficient for the $l$-radiation. The change in the system represented by (11) is given by

$$\varDelta I_1=-\frac{\kappa_l}{4}\varDelta z(2I_1\cos^2\psi-V\cos\psi)\,, \tag{13, a}$$

$$\varDelta I_2=-\frac{\kappa_l}{4}\varDelta z(2I_2-V\cos\psi)\,, \tag{13, b}$$

($l$-absorption)

$$\varDelta U=-\frac{\kappa_l}{4}\varDelta zU(1+\cos^2\psi)\,, \tag{13, c}$$

and

$$\varDelta V=-\frac{\kappa_l}{4}\varDelta z[-2I_1\cos\psi-2I_2\cos\psi+(1+\cos^2\psi)V]\,. \tag{13, d}$$

Quite similarly, we have for the $r$-radiation

$$\varDelta I_1=-\frac{\kappa_r}{4}\varDelta z[2I_1\cos^2\psi+V\cos\psi]\,, \tag{14, a}$$

$$\varDelta I_2=-\frac{\kappa_r}{4}\varDelta z[2I_2+V\cos\psi]\,, \tag{14, b}$$

($r$-absorption)

$$\varDelta U=-\frac{\kappa_r}{4}\varDelta zU(1+\cos^2\psi)\,, \tag{14, c}$$

and

$$\varDelta V=-\frac{\kappa_r}{4}\varDelta z[2I_1\cos\psi+2I_2\cos\psi+(1+\cos^2\psi)V]\,. \tag{14, d}$$

The equations (6), (13) and (14) give the expressions of the selective absorption.

Where $\kappa_p$, $\kappa_l$ and $\kappa_r$ are all equal to $\kappa$, we have

$$\Delta I_1 = -\kappa \Delta z I_1 , \tag{15, a}$$

$$\Delta I_2 = -\kappa \Delta z I_2 , \tag{15, b}$$

(continuous absorption)

$$\Delta U = -\kappa \Delta z U , \tag{15, c}$$

and

$$\Delta V = -\kappa \Delta z V . \tag{15, d}$$

The expressions (15) represent the unpolarized absorption which is the continuous absorption when $\kappa$ means the continuous absorption coefficient.

According to the equations (6), (13), (14) and (15), the total absorption is given by

$$\Delta I_1 = -\kappa \Delta z \left[ \left( 1 + \eta_p \sin^2 \psi + \frac{\eta_l + \eta_r}{2} \cos^2 \psi \right) I_1 + \frac{-\eta_l + \eta_r}{4} \cos \psi V \right] , \tag{16, a}$$

$$\Delta I_2 = -\kappa \Delta z \left[ \left( 1 + \frac{\eta_l + \eta_r}{2} \right) I_2 + \frac{-\eta_l + \eta_r}{4} \cos \psi V \right] , \tag{16, b}$$

$$\Delta U = -\kappa \Delta z \left[ 1 + \frac{\eta_p}{2} \sin^2 \psi + \frac{\eta_l + \eta_r}{4} (1 + \cos^2 \psi) \right] U , \tag{16, c}$$

and

$$\Delta V = -\kappa \Delta z \left[ \frac{-\eta_l + \eta_r}{2} \cos \psi (I_1 + I_2) + \left\{ 1 + \frac{\eta_p}{2} \sin^2 \psi + \frac{\eta_l + \eta_r}{4} (1 + \cos^2 \psi) \right\} V \right] , \tag{16, d}$$

where $\eta_p$, $\eta_l$ and $\eta_r$ denote $\kappa_p/\kappa$, $\kappa_l/\kappa$ and $\kappa_r/\kappa$, respectively.

Next we consider the emission. For simplicity, the pure absorption model is assumed. This approximation may be a good one, because the Zeeman triplets which are usually observed are of moderate strength and moreover the atoms are complex and have many energy levels.

Taking account of the proper polarizations of the $p$-, $l$- and $r$-radiations and the continuous random emission, we have

$$\Delta I_1 = \kappa_p \Delta z \sin^2 \psi \frac{B}{2} , \quad \Delta I_2 = 0 , \quad \Delta U = 0 \quad \text{and} \quad \Delta V = 0 , \tag{17}$$

for the $p$-emission,

$$\Delta I_1 = \kappa_l \Delta z \frac{\cos^2 \psi}{2} \frac{B}{2} , \qquad \Delta I_2 = \kappa_l \Delta z \frac{1}{2} \frac{B}{2} ,$$

$$\Delta U = 0, \qquad \text{and} \qquad \Delta V = -\kappa_l \Delta z \frac{\cos \psi}{2} B , \tag{18}$$

for the $l$-emission,

$$\Delta I_1=\kappa_r\Delta z\frac{\cos^2\psi}{2}\frac{B}{2}, \qquad \Delta I_2=\kappa_r\Delta z\frac{1}{2}\frac{B}{2},$$

$$\Delta U=0, \qquad \text{and} \qquad \Delta V=\kappa_r\Delta z\frac{\cos\psi}{2}B, \tag{19}$$

for the $r$-emission and

$$\Delta I_1=\kappa\Delta z\frac{B}{2}, \quad \Delta I_2=\kappa\Delta z\frac{B}{2}, \quad \Delta U=0, \quad \text{and} \quad \Delta V=0, \tag{20}$$

for the continuous emission. Therefore the total emission is given by

$$\Delta I_1=\kappa\Delta z\left[1+\eta_p\sin^2\psi+\frac{\eta_l+\eta_r}{2}\cos^2\psi\right]\frac{B}{2}, \tag{21, a}$$

$$\Delta I_2=\kappa\Delta z\left[1+\frac{\eta_l+\kappa_r}{2}\right]\frac{B}{2}, \tag{21, b}$$

$$\Delta U=0, \tag{21, c}$$

and

$$\Delta V=\kappa\Delta z\frac{-\eta_l+\eta_r}{2}\cos\psi B. \tag{21, d}$$

It is noted here that the Stokes parameter $U$ has no interaction with other parameters and that $\Delta U$ vanishes in the emission processes. Therefore $U$ is identically zero,

$$U=0. \tag{22}$$

We need only to treat the equations of transfer for three parameters, which are written from equation (16) and (21) as

$$\cos\theta\frac{dI_1}{d\tau}=\left(1+\eta_p\sin^2\psi+\frac{\eta_l+\eta_r}{2}\cos^2\psi\right)\left(I_1-\frac{B}{2}\right)+\frac{-\eta_l+\eta_r}{4}\cos\psi V,$$

$$\cos\theta\frac{dI_2}{d\tau}=\left(1+\frac{\eta_l+\eta_r}{2}\right)\left(I_2-\frac{B}{2}\right)+\frac{-\eta_l+\eta_r}{4}\cos\psi V,$$

and

$$\cos\theta\frac{dV}{d\tau}=\frac{-\eta_l+\eta_r}{2}\cos\psi(I_1+I_2-B)+\left\{1+\frac{\eta_p}{2}\sin^2\psi+\frac{\eta_l+\eta_r}{4}(1+\cos^2\psi)\right\}V,$$

where

$$d\tau=-\kappa dz\sec\theta. \tag{23}$$

These equations reduce to

$$\cos\theta\frac{dI}{d\tau}=(1+\eta_I)I+\eta_Q Q+\eta_V V-(1+\eta_I)B\,, \tag{24}$$

$$\cos\theta\frac{dQ}{d\tau}=\eta_Q I+(1+\eta_I)Q-\eta_Q B\,, \tag{25}$$

and

$$\cos\theta\frac{dV}{d\tau}=\eta_V I+(1+\eta_I)V-\eta_V B\,, \tag{26}$$

where

$$I=I_1+I_2\,,\qquad Q=I_1-I_2\,,$$

$$\eta_I=\frac{\eta_p}{2}\sin^2\psi+\frac{\eta_l+\eta_r}{4}(1+\cos^2\psi)\,, \tag{27, a}$$

$$\eta_Q=\left(\frac{\eta_p}{2}-\frac{\eta_l+\eta_r}{4}\right)\sin^2\psi\,, \tag{27, b}$$

and

$$\eta_V=\frac{-\eta_l+\eta_r}{2}\cos\psi\,. \tag{27, c}$$

As the functional forms of $\eta_p$, $\eta_l$ and $\eta_r$ have not been specified in the deduction of the equations (24), (25) and (26), these simultaneous equations can be used also for the lines with the anomalous Zeeman effect. In that case, the equations (3) have to be disregarded and, instead, the special partition of the absorption coefficients for these lines has to be adopted. But the anomalous Zeeman effect will not be considered in detail in this paper.

## 3. *The Solution of the Equations of Transfer.*

Assuming the homogeneous magnetic field and neglecting the variations of $\eta_p$, $\eta_l$ and $\eta_r$ with the optical depth, we can solve the equations (24), (25) and (26) easily. Putting

$$B=B_0(1+\beta_0\tau)\,, \tag{28}$$

we obtain the emergent intensities,

$$I(0,\theta)=B_0\left[1+B_0\cos\theta\,\frac{1+\eta_I}{(1+\eta_I)^2-\eta_Q^2-\eta_V^2}\right], \tag{29, a}$$

$$Q(0,\theta)=-B_0\beta_0\cos\theta\,\frac{\eta_Q}{(1+\eta_I)^2-\eta_Q^2-\eta_V^2}\,, \tag{29, b}$$

and

$$V(0,\theta)=-B_0\beta_0\cos\theta\,\frac{\eta_V}{(1+\eta_I)^2-\eta_Q^2-\eta_V^2}\,. \tag{29, c}$$

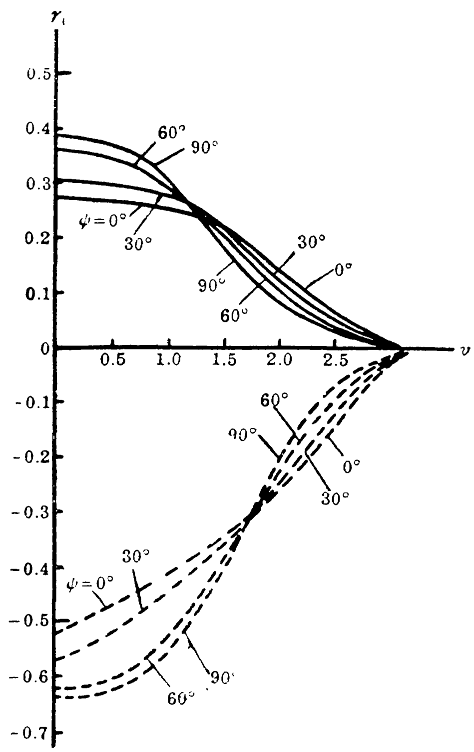


Fig. 2–a

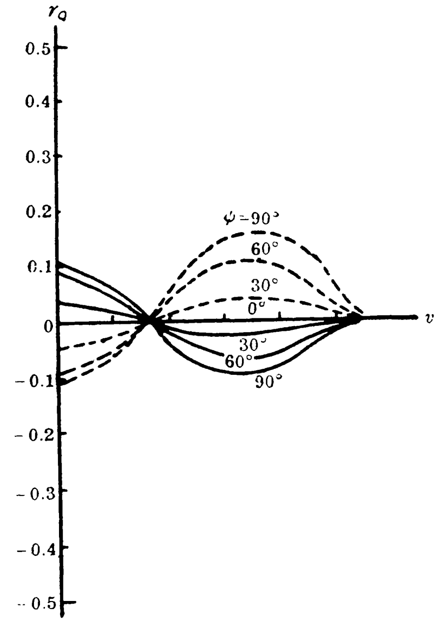


Fig. 2–b

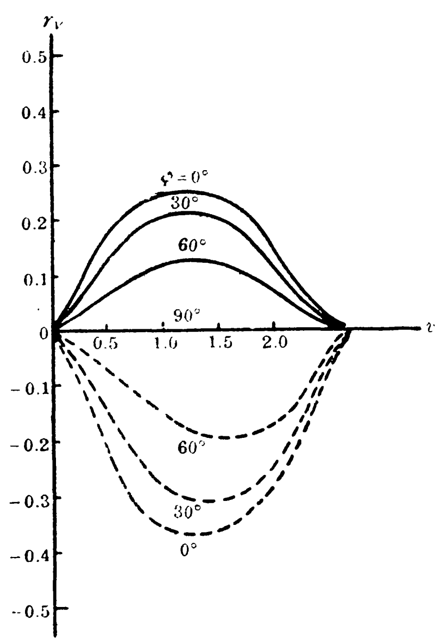


Fig. 2–c

Fig. 2. Depressions of the Stokes parameters in the equations (31) for $v_H=1$ and for $\psi=0°, 30°, 60°$ and 90°. Full lines and dashed lines represent for the cases of $\eta_0=1$ and $\eta_0=3$ respectively, in the equations (33). (a) $r_I$, (b) $r_Q$ and (c) $r_V$.

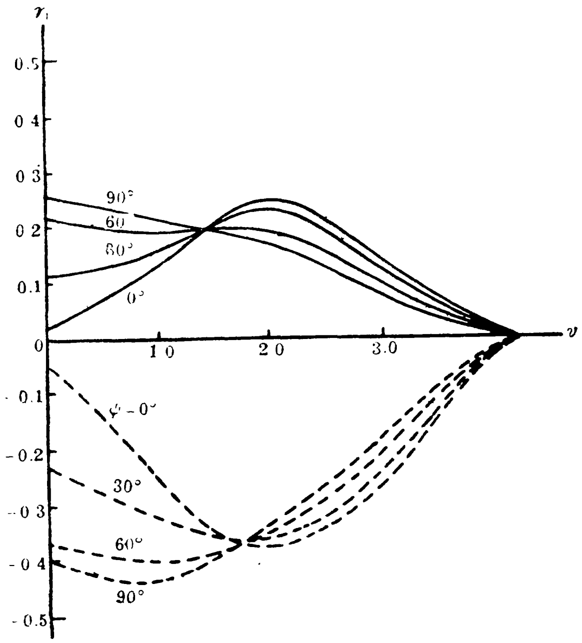


Fig. 3-a

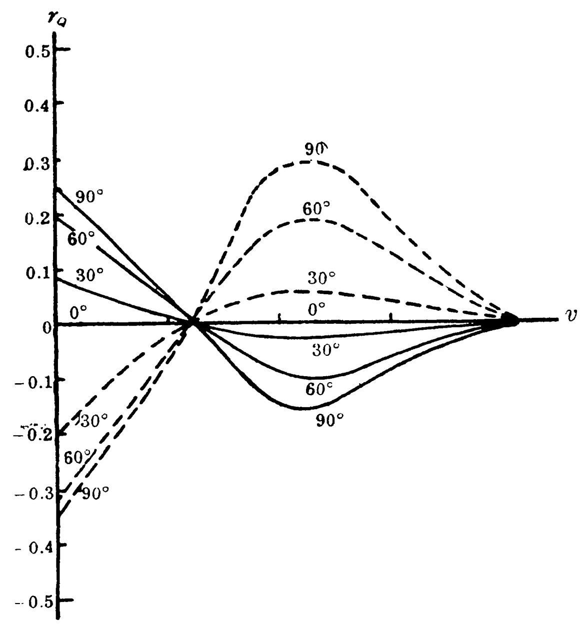


Fig. 3-b

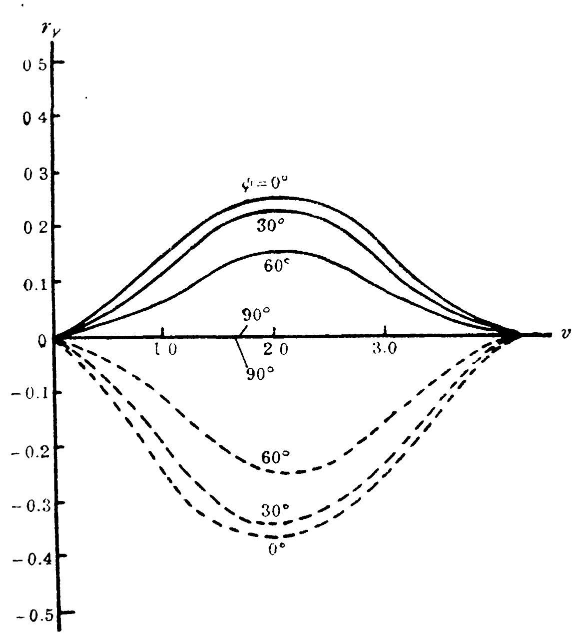


Fig. 3-c

Fig. 3. Depressions of the Stokes parameters in the equations (31) for $v_H=2$ and for $\psi=0°$, 30°, 60° and 90°. Full lines and dashed lines represent for the cases of $\eta_0=1$ and $\eta_0=3$, respectively, in the equations (33). (a) $r_I$, (b) $v_Q$ and (c) $r_V$.

In Figs. 2 and 3, only the right halves of the contours are shown because of the symmetry. The curves for $\eta_0=3$ are drawn by changing the sign of $r_I$, $r_Q$ and $r_V$. $r_I$ and $r_Q$ are symmetric with respect to the axis $v=0$, and $r_V$ is symmetric with respect to the origin.

For the continuous back ground, we put

$$\eta_p = \eta_l = \eta_r = 0 \quad \text{or} \quad \eta_I = \eta_Q = \eta_V = 0 ,$$

and we have

$$I_0(0, \theta) = B_0(1 + \beta_0 \cos \theta) , \tag{30, a}$$

$$Q_0(0, \theta) = 0 , \tag{30, b}$$

and

$$V_0(0, \theta) = 0 . \tag{30, c}$$

The intensities and the polarization of the absorption line are measured in units of the continuous back ground, so that

$$r_I(\theta) = \frac{I_0(0, \theta) - I(0, \theta)}{I_0(0, \theta)} = \frac{\beta_0 \cos \theta}{1 + \beta_0 \cos \theta} \left[ 1 - \frac{1 + \eta_I}{(1 + \eta_I)^2 - \eta_Q^2 - \eta_V^2} \right] , \tag{31, a}$$

$$r_Q(\theta) = \frac{Q_0(0, \theta) - Q(0, \theta)}{I_0(0, \theta)} = \frac{\beta_0 \cos \theta}{1 + \beta_0 \cos \theta} \, \frac{\eta_Q}{(1 + \eta_I)^2 - \eta_Q^2 - \eta_V^2} , \tag{31, b}$$

and

$$r_V(\theta) = \frac{V_0(0, \theta) - V(0, \theta)}{I_0(0, \theta)} = \frac{\beta_0 \cos \theta}{1 + \beta_0 \cos \theta} \, \frac{\eta_V}{(1 + \eta_I)^2 - \eta_Q^2 - \eta_V^2} \tag{31, c}$$

If we ignore the effect of polarization altogether, we have

$$Q = V = 0 ,$$

or equivalently

$$\eta_Q = \eta_V = 0 ,$$

and the equation (31, a) is reduced to

$$r_I(\theta) = \frac{\beta_0 \cos \theta}{1 + \beta_0 \cos \theta} \, \frac{\eta_I}{1 + \eta_I} \tag{32}$$

As the contour of the absorption coefficient is widened by the Zeeman effect, we have a large magnetic intensification. But in the actual cases, the polarizations of the $p$-, $l$- and $r$-oscillators are not identical and so the correction $-(\eta_Q^2 + \eta_V^2)$ appears in the denominator of the equation (31, a). As the result, the magnetic intensification is somewhat less than that calculated from the equation (32).

Numerical calculations have been made for the representative cases and are shown in Figs. 2 and 3. Assuming the Doppler contour, we have

$$\eta_p = \eta_0 e^{-v^2} , \quad \eta_l = \eta_0 e^{-(v - v_H)^2} \quad \text{and} \quad \eta_r = \eta_0 e^{-(v + v_H)^2} , \tag{33}$$

where $v$ and $v_H$ measure the wave-length and the wave-length shift due to the Zeeman effect in units of the Doppler half width, respectively. $\eta_0=1$ and $\eta_0=3$, and $v_H=1$ and $v_H=2$ are adopted in the calculations. $r_I$, $r_Q$ and $r_V$ are shown in Figs. (2a) and (3a), (2b) and (3b) and (2c) and (3c), respectively, for 0°, 30°, 60° and 90°. For $\psi>90°$, the results for $180°-\psi$ can be obtained only by exchanging the roles of the $l$- and the $r$-oscillators. So, we shall restrict the later discussions for $0°<\psi<90°$ without loss of generality.

## 4. *Discussions about Some Special Cases.*

In the cases of the longitudinal and the transverse normal Zeeman effects, the angle $\psi$ is 0° and 90°, respectively.

From the equations (27, a, b, c) and (31, a, b, c) we have for $\psi=0°$,

$$r_I=\frac{\beta_0\cos\theta}{1+\beta_0\cos\theta}\frac{1}{2}\left[\frac{\eta_l}{1+\eta_l}+\frac{\eta_r}{1+\eta_r}\right], \tag{34, a}$$

$$r_Q=0\,, \tag{34, b}$$

and

$$r_V=\frac{\beta_0\cos\theta}{1+\beta_0\cos\theta}\frac{1}{2}\left[-\frac{\eta_l}{1+\eta_l}+\frac{\eta_r}{1+\eta_r}\right], \tag{34, c}$$

and for $\psi=90°$,

$$r_I=\frac{\beta_0\cos\theta}{1+\beta_0\cos\theta}\frac{1}{2}\left[\frac{\eta_p}{1+\eta_p}+\frac{(\eta_l+\eta_r)/2}{1+(\eta_l+\eta_r)/2}\right], \tag{35, a}$$

$$r_Q=\frac{\beta_0\cos\theta}{1+\beta_0\cos\theta}\frac{1}{2}\left[\frac{\eta_p}{1+\eta_p}-\frac{(\eta_l+\eta_r)/2}{1+(\eta_l+\eta_r)/2}\right], \tag{35, b}$$

and

$$r_V=0\,. \tag{35, c}$$

The equations (34) and (35) are consistent with the formulae given by Hubenet. From equations (3), (34, a) and (35, a), we have no magnetic intensification in the case of the longitudinal normal Zeeman effect, but we have an appreciable magnetic intensification in the case of the transverse normal Zeeman effect, because $\eta_l$ and $\eta_r$ have their maxima at the different wave-lengths and the saturation effect of the equivalent width becomes less marked. When the Zeeman components are well separated, the formula (31, a) can be divided into three terms e.g.,

$$r_I=\frac{\beta_0\cos\theta}{1+\beta_0\cos\theta}\frac{1}{2}\left[\frac{\eta_p\sin^2\psi}{1+\eta_p\sin^2\psi}+\frac{\eta_l(1+\cos^2\psi)/2}{1+\eta_l(1+\cos^2\psi)/2}+\frac{\eta_r(1+\cos^2\psi)/2}{1+\eta_r(1+\cos^2\psi)/2}\right]. \tag{36}$$

The equivalent width $W$ is given by

$$\frac{W}{\Delta\lambda_D}=\int_{-\infty}^{+\infty} r_I dv\,, \tag{37}$$

where $v$ denotes the wave-length shift in units of Doppler width $\Delta\lambda_D$. The equations (36) and (37) show that $W$ is maximum when

$$\sin^2\psi=(1+\cos^2\psi)/2\,,$$

or

$$\cos^2\psi=1/3\,. \tag{38}$$

Therefore we expect the maximum magnetic intensification when the angle $\psi$ is near 55° (or 125°). Numerical calculations or Figs. 2 and 3 show that the equivalent width $W$ increases rapidly with increasing $\psi$ until $\psi$ becomes about 55° however after that it remains to be practically constant, although the contours of $r_I$, $r_Q$ and $r_V$ show marked variations with $\psi$.

Next, when the magnetic field is so weak that the higher order in $v_H$ can be neglected, we have

$$\eta_p=\eta(v)\,,\qquad \eta_l=\eta(v-v_H)=\eta(v)-v_H\frac{d\eta}{dv}\,,$$

and

$$\eta_r=\eta(v+v_H)=\eta(v)+v_H\frac{d\eta}{dv}\,. \tag{39}$$

From the equations (27, a, b, c),

$$\eta_I=\eta(v)\,,\qquad \eta_Q=0\qquad \text{and}\qquad \eta_V=v_H\cos\psi\frac{d\eta}{dv}\,. \tag{40}$$

As we shall see later, the usual observation by means of a quater-wave plate and a polarizer measures $r_I\pm r_V$, which is given from (40) in the case of infinitesimal splitting by

$$r_I\pm r_V=\frac{\beta_0\cos\theta}{1+\beta_0\cos\theta}\,\frac{\eta(v\pm v_H\cos\psi)}{1+\eta(v\pm v_H\cos\psi)}\,. \tag{41}$$

This formula is the same as in the case of the longitudinal Zeeman effect where the magnetic field strength is multiplied by a factor $\cos\psi$. The formula (41) was first derived by F. H. Seares[9] although his treatment was not exact, for he assumed that each Zeeman component forms the absorption line of the same symmetrical shape apart from the magnitude of the depression. Anyhow Seares' formula is useful for the measurement of the weak general magnetic field.

Next, a discussion about the curve of growth of a sun-spot will be made. As we see from Figs. 2a and 3a, the magnetic intensification is at most of the order of 10 per cent or more if $\eta_0$ is fairly large. In the case of the normal Zeeman triplet, the magnetic intensification is expected when the magnetic line of force makes an appreciable angle with the line of sight or when the effect of the atmospheric scintillation is so large that the scattered light from the penumbra modifies the spectrum of the umbra appreciably. If the observations of ten Bruggencate and von Klüber[5] were made about the sun-spot near the center of the sun in good seeing, the magnitude of the magnetic intensification might be below 5 per cent. So, ten Bruggencate and von Klüber's value of about 80 per cent seems to be too large. Warwick[7] made the curve of growth by using only the lines with the normal Zeeman triplet and found that no systematic deviation from the curve exists for the lines with the anomalous Zeeman effect. He interpreted the result by means of the turbulent velocity of 2 km/sec which overcomes the magnetic broadening. But many anomalous Zeeman patterns show grouping, although there are some exceptions. So, these lines show no marked differences with the normal Zeeman lines in the spectrum of the sun-spot, and their magnetic intensification may be small. Michard[6] showed that the anomalies of the sun-spot curve of growth disappears in the "Fein Analyse". Therefore, the turbulent motion of 2 km/sec, which is doubtful in the presence of the strong magnetic field, may be not real. Anyhow the detailed study of the line contour will solve the problem of the curve of growth.

## 5. *The Observational Scheme.*

The observations of the Zeeman patterns are made by using the quartz or the mica plate and the analyzer combined with the spectrograph. Fig. 4 shows the relation of the coordinate systems. The $x$- and $y$-axes give the coordinates which have hitherto been used. The principal axes of the fast and the slow electric vibrations are indicated by $f$ and $s$, respectively, and the angle which the $f$-axis makes with the $x$-axis is denoted by $\phi$. The X- and Y-axes mean the directions of the ordinary and the extraordinary vibration of the analyzing double image prism, and the X-axis should make an angle 45° with the $f$-axis.

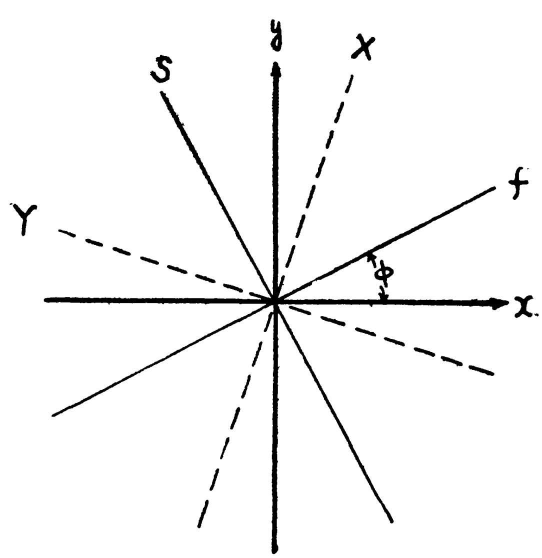


Fig. 4. Directions of the axes of the quartz and the analyzer.

The light which is represented by the system (1) or (2) is affected by the crystal plate and the analyzer in such a way that

$$\xi_f = \xi_1 \cos(\omega t - \epsilon_1)\cos\phi + \xi_2 \cos(\omega t - \epsilon_2)\sin\phi\,, \qquad (42,\ a)$$

$$\xi_s = \xi_1 \cos(\omega t - \epsilon_1 - \delta)\sin\phi + \xi_2 \cos(\omega t - \epsilon_2 - \delta)\cos\phi\,, \qquad (42,\ b)$$

$$\xi_X = \frac{1}{\sqrt{2}}(\xi_f + \xi_s), \tag{43, a}$$

and

$$\xi_Y = \frac{1}{\sqrt{2}}(-\xi_f + \xi_s), \tag{43, b}$$

where $\delta$ means the phase retardation produced by the crystal.

After passing the analyzing double image prism, the intensities of the ordinary and the extraordinary rays become

$$I_{X,\delta} = \frac{1}{2}[I - Q\sin 2\phi\cos\delta + U\cos\delta\cos 2\phi + V\sin\delta], \tag{44, a}$$

and

$$I_{Y,\delta} = \frac{1}{2}[I + Q\sin 2\phi\cos\delta - U\cos 2\phi\cos\delta - V\sin\delta], \tag{44, b}$$

from the equations (2), (42) and (43). In our case,

$$U = 0. \tag{22}$$

And if the half-wave plate and the quater-wave are used,

$$\delta = n\pi \quad \text{and} \quad \delta = n\pi + \frac{1}{2}\pi, \quad \text{respectively,}$$

and the equations (44) reduce to

$$I_{X,0} = \frac{1}{2}[I - Q\sin 2\phi], \tag{45, a}$$

$$I_{Y,0} = \frac{1}{2}[I + Q\sin 2\phi], \tag{45, b}$$

$$I_{Y,\pi/2} = \frac{1}{2}[I + V], \tag{45, c}$$

and

$$I_{Y,\pi/2} = \frac{1}{2}[I - V]. \tag{45, d}$$

If the scattered light can be neglected, we have in terms of depressions,

$$r_{X,0} = r_I - r_Q\sin 2\phi,$$

$$r_{Y,0} = r_I + r_Q\sin 2\phi,$$

$$r_{X,\pi/2} = r_I + r_V,$$

and

$$r_{Y,\pi/2} = r_I - r_V,$$

or

$$r_I=\frac{1}{2}(r_{X,0}+r_{Y,0})=\frac{1}{2}(r_{X,\pi/2}+r_{Y,\pi/2}), \qquad (46, a)$$

$$r_Q\sin 2\phi=\frac{1}{2}(-r_{X,0}+r_{Y,0}), \qquad (46, b)$$

and

$$r_V=\frac{1}{2}(r_{X,\pi/2}-r_{Y,\pi/2}). \qquad (46, c)$$

The quantities appeared in the right-hand sides of the equations (46) are the observable ones, and $r_I$, $r_Q$ and $r_V$ on the left hand sides are given by the expressions (31) and (27). Adopting the Doppler contour of the absorption coefficient such as represented by the equations (33), the unknown quantities in the equations (46) are $\beta_0$, $\eta_0$, $v_H$, $\psi$ and $\phi$. The value of $\beta_0$ is given by the Michard's[6] study, and then the value of $\eta_0$ is determined mainly by the observed value of $r_I$ which is sensitive to the variation of $\eta_0$ as seen from Figs. 2 and 3. The value of $v_H$ is then determined by the wave length at which $r_V$ shows its maximum. With the values of $\beta_0$, $\eta_0$ and $v_H$ thus obtained, the angles $\psi$ and $\phi$ can be determined by the values of $r_V/r_I$ and $r_Q\sin 2\phi/r_I$. The values of $\psi$ and $\phi$ are obtained from the observations at one wave-length in the contour, and the consistency of them from the observations at different wave-length checks the adopted values of $\beta_0$, $\eta_0$ and $v_H$. These angles indicate the orientation of the magnetic field at any point of a sun-spot along the slit of the spectrograph.

Actually, the observations of sun-spots always suffer from the scattered light mainly due to the atmospheric scintillation. The scattering function may be assumed after A. J. M. Wanders[10] to be

$$U(x, y)=\frac{a}{\pi}e^{-a(x^2+y^2)}, \qquad (47)$$

The observational quantities are here written symbolically as

$$I_{Obs}=(1-s)I+sI_s, \qquad (48, a)$$

$$Q_{Obs}=(1-s)Q+sQ_s, \qquad (48, b)$$

and

$$V_{Obs}=(1-s)V+sV_s, \qquad (48, c)$$

where $I_{Obs}$, $Q_{Obs}$ and $V_{Obs}$ means the quantities which reach the observational instruments. $I$, $Q$ and $V$ should mean the quantities in the area where the magnetic field and other physical quantities are regarded as uniform, and $I_s$, $Q_s$ and $V_s$ mean the effective quantities scattered from the surrounding area. The magnitude of scattering, $s$ and $I_s$, $Q_s$ and $V_s$ can be written by means of the scattering function (47), if the size of the uniform area is adopted.

Defining the following quantities

$$p=\frac{1-s}{1-s(1-I_{0s}/I_0)}, \tag{49, a}$$

$$q=\frac{s}{1-s(1-I_{0s}/I_0)}, \tag{49, b}$$

where $I_0$ and $I_{0s}$ are the corresponding quantities for the continuous back ground, we have

$$pr_I+qr_{Is}=\frac{1}{2}(r_{X,\pi/2}+r_{Y,\pi/2}), \tag{50, a}$$

$$(pr_Q+qr_{Qs})\sin 2\phi=\frac{1}{2}(-r_{X,0}+r_{Y,0}), \tag{50, b}$$

and

$$pr_V+qr_{Vs}=\frac{1}{2}(r_{X,\pi/2}-r_{Y.\pi/2}). \tag{50, c}$$

The distributions of the intensity and the polarization along the line contour are different if the strength and the orientation of magnetic field are different. Therefore, we can distinguish the component of scattered light. For instance, the scattered light from the normal photosphere has random polarization and the absorption line is confined only near the line centre and is not widened by the Zeeman effect, and so the intensity and the polarization are scarecely affected at the wave-length somewhat apart from the line center. We can determine the magnitude of $s$ in this case empirically by observing the intensity and the polarization near the line center.

In the actual procedure, the successive approximation may be most convenient, first taking the umbra and the penumbra of the sun-spot as the uniform areas and obtaining the parameters and then subdividing the areas smaller and smaller and finally a precise distrubution of the magnetic field across the sun-spot will be obtained.

If the scattering parameter $s$ is applied to the continuous spectrum the intensity distribution across the sun-spot will be obtained.

It is important to note here that the observation must be made by a single exposure, for the scintillation varies with time. For this purpose, a quartz plate which can serve as a quarter-wave plate for one line and as a half-wave plate for the other line simultaneously is favorable. The iron lines $\lambda$ 6303 and $\lambda$ 6173 are adequate for the observation, for these lines have large Landé factors and the effective depths where the lines are formed are nearly the same. A vanadium line $\lambda$ 6259 which is situated between the iron lines is a weaker line and the effective depth is deeper. And so, if the line contour is also measured, some information about the variation of the magnetic field with depth can be obtained. The relation, curl $H=0$, together with the observation of these lines may well determine the three dimensional structure of the sun-spot magnetic field. Such an observation is now undertaken at the Tokyo Astronomical Observatory.

In the case of magnetic stars we need not take care of the atmospheric scintillation, but instead, $r_I(\theta)$, $r_Q(\theta)$ and $r_V(\theta)$ must be integrated over the stellar disc. As the strength and the orientation of magnetic field are the functions of position on the disc, the interpretation of the observed contour may require a somewhat complicated calculation. However, it may be interesting to test by the detailed study whether the magnetic field of the star is the general dipole field or it it is due to large magnetic spots.

The auther expresses his hearty thanks to Dr. Z. Suemoto and Mr. S. Hokugo for their kind encouragement and discussions.

## References


1) H. W. Babcock, *Ap. J.*, **110**, 126, 1949.
2) H. Hubenet, *Zs. f. Ap.*, **34**, 110, 1954.
3) J. Houtgast and A. van Sluiters, *B.A.N.*, **10**, 325, 1948.
4) G. E. Hale, F. Ellerman, S. B. Nicholson and A. H. Joy, *Ap. J.*, **49**, 153, 1919.
5) P. ten Bruggencate and H. von Klüber, *Zs. f. Ap.*, **18**, 284, 1939.
6) R. Michard, *Ann. d'Ap.*, **16**, 217, 1953.
7) J. Warwick, *Zs. f. Ap.*, **35**, 245, 1954.
8) S. Chandrasekhar, *Radiative Transfer*. Oxford Univ. Press, 1950.
9) F. H. Seares, *Ap. J.*, **38**, 99, 1913.
10) A. J. M. Wanders, *Zs. f. Ap.*, **8**, 108, 1934.